Application of Frequency Control Techniques for Hot Tensile Testing in Induction Heating

Saichol Chudjuarjeen[1] and **Nathabhat Phankong**[2†], Non-members

ABSTRACT

This paper proposes the frequency control technique using a half-bridge resonance inverter for hot tensile testing in induction heating. The technique involves power regulation, high frequency pulse, frequency adjustment, and pulse generator controller based on the dsPIC33FJ16GS404 chip IC. Significantly, the inverter is controlled by two sections. Throughout the heating cycle, the first controller retains the inverter's operating frequency slightly above the resonant frequency, while the second keeps the phase angle of the current and voltage output in check to control the output power at a level suitable for changes in the tensile parameter workpieces. As a result, the inverter improves the efficiency of the prototype, which has 1.5 kW input power. Furthermore, it can heat three different sizes of steel workpieces for hot tensile testing, with diameters of approximately 3, 5, and 10 mm and lengths of approximately 50 and 70 mm, respectively.

Keywords: Half-bridge Inverter, Frequency Control Technique, Pulse Width Modulation, PWM, Hot Tensile Testing

1. INTRODUCTION

Induction heating is now widely used in the treatment of workpieces such as hardening, forging, brazing, and welding [1], with each operation requiring a distinct frequency and power for melting. The shape and size of the workpieces, as well as the desired crucible depth, determine the frequency and power employed. The appropriate temperature of the entire workpiece must be reached during the heating process. A magnetic field is formed around the coil as electric current flows through it and then reversed according to the frequency of the alternating current [2–6]. Furthermore, the magnetic field cuts through the iron in reverse polarity when placed in the coil. This generates an electric current in the steel, known as eddy current. However, the eddy current is not uniform across the cross-sectional area of the steel bar but occurs on the surface of the iron. The electric current grows more powerful along the surface as the frequency of the electric current rises. This is referred to as the skin effect. It produces heat for hardening steel by heating it to a critical temperature of about 780–950 ℃ and then rapidly cooling it down beyond the critical cooling rate with water or oil to elicit structural changes in the steel. It is also used in surface hardening applications, employing a semiconductor as a switch to operate the inverter circuit. This progression can be used as a load current source or a series resonant load voltage source. For improved sufficiency, a voltage source inverter used in electrical induction heating can be used to match the resonance in applications where the power is not too high. Two types of inverters are installed into high frequency induction heaters: voltage source and current source. In the past, series and parallel resonant inverter circuits were used in conjunction with half-bridge and full-bridge to reduce switching loss and increase circuit efficiency [7–17].

Several resonant inverters for induction heating applications have been proposed. Chudjuarjeen proposed a high-frequency induction cooker using a quasi-resonant converter [2]. The converter had fewer switches than other types and fewer switching losses than half-bridge and full-bridge inverter circuits. Throughout the switching frequency, the suggested input power control technique allows the switch to function under zero-voltage switching conditions. The switch is tough to manipulate making it vulnerable to damage. Chudjuarjeen presented the asymmetrical control of a series resonant inverter with a phase-locked loop, utilizing full-bridge circuits in an induction heating stove [3–4]. It can modify the output power of the induction cooker by altering the asymmetrical control using the duty cycle PWM control signal, while the switch operates under ZVS conditions, thereby reducing circuit switch loss. Chudjuarjeen proposed an LLC resonant inverter for induction heating applications with asymmetrical control [5–6]. An asymmetrical control technique with a phase-locked loop can be used to manage the switching frequency and phase current. According to the simulation results, when comparing the experimental results with the test circuit operation, the switching frequency is extremely high in this circumstance. However, there is a possibility that the switch will be damaged due to turn-on and turn-off errors. Polsripim proposed a soft switching class

Manuscript received on September 1, 2021; revised on October 16, 2021; accepted on October 19, 2021. This paper was recommended by Associate Editor Yuttana Kumsuwan.

[1]The author is with the Department of Electrical Engineering, Faculty of Engineering, Rajamangala University of Technology Krungthep, Bangkok, Thailand.

[2]The author is with the Department of Electrical Engineering, Faculty of Engineering, Rajamangala University of Technology Thanyaburi, Pathum Thani, Thailand.

[†]Corresponding author: nathabhat_p@rmutt.ac.th

Digital Object Identifier: 10.37936/ecti-eec.2022201.246110

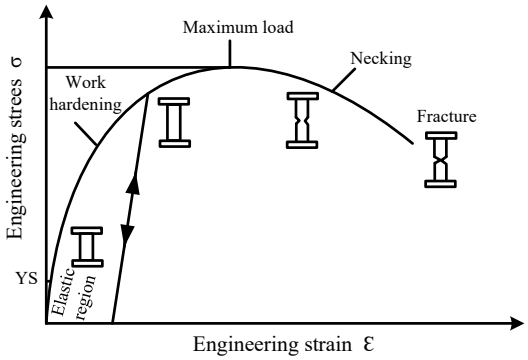

Fig. 1: *Standard cylindrical test specimen with a stress-strain curve [18].*

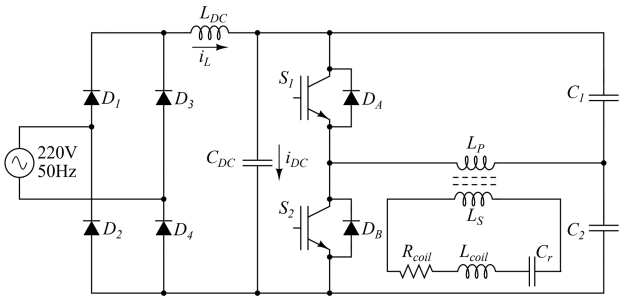

Fig. 2: *Proposed circuit for hot tensile testing.*

D current source inverter for induction heating with a ferromagnetic load [7]. The prototype has a power of 1.26 kW and a temperature of 680 ℃. It uses a half-bridge class D current source inverter circuit, which employs fewer switches than a full-bridge inverter circuit, resulting in fewer switching and conduction losses. The switching frequency is very high. There is a chance of errors during turn-on and turn-off conditions. Samart proposed an automatic half-bridge resonant inverter with a three-phase, three-switch buck-type rectifier [8]. A 1.5 kW inverter is used in the design of a half-bridge circuit for induction heating. The circuit operates under zero-voltage switching conditions, has a constant turn-off time across the switching frequency, and uses fewer switches than the full-bridge system . As a result, switching losses are lower than with a full-bridge system. The control circuits for the converter and inverter, on the other hand, are separate. This makes it more difficult to operate both circuits since the system relies on many switches to function, resulting in significant switching losses. Jittakort proposed the variable frequency asymmetrical voltage cancellation control of a series resonant inverter [9–11]. The output power of the full-bridge inverter circuit is regulated via asymmetrical control frequency adjustment for series resonant loads. The asymmetrical control is fully automated and operates under zero-voltage switching conditions. As a result, the circuit has negligible switching losses.

The hot tensile test (HTT) is a technique for determining the material properties at high temperatures. In applications, such as aerospace and automotive, its high-temperature qualities are significant drawbacks. Many components, including pistons, valves, and cylinder heads, are exposed to high temperatures, resulting in thermal stress and component failure. Consequently, it is critical that the impact of high temperatures on material strength be investigated. Using a furnace and an extensometer on the test specimen, tensile heating is a suitable method for tensile testing [18–19]. The tensile heating method can be used to determine the tensile strength, elongation, and strength of a variety of materials as well as high-temperature alloys. Furthermore, the test pieces can be cylindrical or flat in shape. Fig. 1 shows a standard typical cylindrical specimen, grasped at both ends and pulled apart in the machine by the application of a load. The stress-strain curve derived from a tensile test on typical ductile metal is shown in Fig. 1. The engineering stress σ is represented on the y-axis, defined as load P divided by the original cross-sectional area A_0 of the test piece. The engineering strain ε depicted on the x-axis is defined as the change in length dL divided by the initial gauge length L_a. The percentage elongation is obtained by multiplying the engineering strain by 100.

As discussed, none of the solutions proposed suitable techniques for hot tensile testing. This paper proposes the use of a half-bridge resonant inverter for induction heating in hot tensile testing applications based on the dsPIC33FJ16GS404 chip IC. A dual phase-locked loop adjusts the duty cycle of the switching devices in the inverter. The controller varies the operating frequency of the inverter throughout the heating cycle at a frequency slightly over the resonant frequency.

2. CIRCUIT DESCRIPTION AND SIMULATION

2.1 Circuit Description

Fig. 2 depicts the systems of the prototype for hot tensile testing. The rectifier in the induction heating machine converts AC to DC electricity for the inverter, receiving a single-phase input voltage of 220 V, 50 Hz. The inverter subsequently converts the DC voltage into a high-frequency AC voltage, which is then fed into the series resonant load unit.

2.2 Resonant Load Unit

For tensile testing, induction heating consists of hollow nonferromagnetic (copper) tubes because copper is a good conductor of electricity and results in low power loss for inductance coils. However, high current density in the inductor coil ensures a highly efficient system. The heat temperature generated by the current flowing into the inductor coil is very high. The waveform of the load current is almost sinusoidal. Consequently, the load has a low damping factor because the circuit operates near to the resonant frequency for simplicity of analysis. The equivalent circuit is shown in Fig. 3 and can be written as

$$V_R + V_L + V_C = V_S. \tag{1}$$

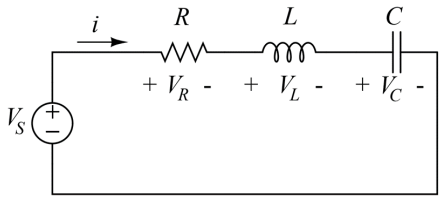

Fig. 3: *Equivalent circuits used in analysis.*

To represent the current-voltage relationship, Eq. (1) can be expressed as

$$iR + L\frac{di}{dt} + \frac{1}{C}\int_0^t idt = V_S. \tag{2}$$

The differential equation of the equivalent circuit can be expressed by

$$\frac{Ld^2i}{dt^2} + \frac{Rdi}{dt} + \frac{i}{C} = \frac{di}{dt}V_S \tag{3}$$

$$\frac{d^2i}{dt^2} + \frac{R}{L}\frac{di}{dt} + \frac{i}{LC} = \frac{1}{L}\frac{di}{dt}V_S \tag{4}$$

The natural angular frequency and damping coefficient reassigned as

$$\omega_0 = \frac{1}{\sqrt{LC}} \tag{5}$$

$$\zeta = \frac{1}{2}\frac{R}{\sqrt{L/C}} \tag{6}$$

The surface resistance of the workpiece $R_s(\Omega)$ is determined by the surface depth of the specimen and its specific resistance, calculated by

$$R_s = \frac{\rho_w}{\delta_w} = \sqrt{\frac{\rho_w \mu_0 \mu_w \omega_s}{2}} \tag{7}$$

where δ_w is the surface depth of the workpiece (m), ρ_w is the specific resistance of the specimen (Ωm), μ_0 is the relative magnetic permeability of air (H/m), μ_w is the relative magnetic permeability of the workpiece (H/m), and ω_s is the angular frequency of the switching (rad/s).

2.3 Controller

The dual phase lock loop control is shown in Fig. 4. It has two loops: main and secondary. The main loop is composed of a current sensor at load, zero-crossing detector, phase shift circuit, lowpass filter 1, phase detector 1, voltage-controlled oscillator (VCO) 1, and PI controller 1. The secondary loop is composed of low pass filter 2, phase detector 2, VCO 2, and PI controller 2. At a slightly higher inverter frequency than the resonant frequency, the phase-locked loop integrated circuit is used for frequency regulation. The phase-locked IC 4046 uses an exclusive-OR gate and VCO. The gate drive signal for the voltage source resonant inverter is in phase with the signal of the load voltage phase. As a result, it is possible to use the VCO 1 output rather than the load voltage pulse. The current signal is compared to the voltage signal to detect the difference in the phase using the exclusive-OR gate, which is well-known for being a phase difference detector. It is necessary to use two IC phase-locked loops in the closed-loop to transport the voltage signal through a zero-crossing detector to shift the phase origin 90 degrees before bringing it into phase detectors 1 and 2. To obtain an average voltage value, the signal from phase detectors 1 and 2 is filtered using an RC low-pass filter. The average voltage reflects the phase difference between voltage and current at load. At that point, the voltage is compared to the required phase set. The input of constant phase controller 1 represents the phase error from the comparison. The output of phase controller 1 is then compared to the output of the phase-locked loop 2 (VCO 2). When the parameters of the heating load are modified, the parameter of this error represents the input of constant phase controller 2 to adjust the VCO to maintain a constant leading phase angle. The control is achieved by sensing the current and voltage induced by the coil via the multiple circuit, then passing the result through an RC low-pass filter to obtain the average power. This is then compared to the set power via a closed-control cycle using a PI controller, as shown in Fig. 4.

The work begins by inserting the workpiece into the inductor coil and adjusting the power, which will result in an error. The controller adjusts the power according to the setting value. The voltage regulator will not command the voltage source to boost the voltage gain after adjusting the power until the value equals the setpoint. The inductor current decreases as the temperature of the workpiece increases. The voltage will be adjusted to the desired power by the controller.

The phase-locked loop structure consists of a feedback system with a VCO for adjusting the frequency in response to the reference signal. The phase comparator, frequency filter, and VCO are the three main components of a phase-locked loop. In a nutshell, it works like this: When an external reference frequency signal is present, the phase capacitor receives a periodic signal. The phases of the reference frequencies are compared to the frequency feedback from the VCO signal. A voltage signal proportional to the phase difference of the two signals will serve as the phase detector. This voltage is then applied to the loop filter circuit, which eliminates undesirable frequencies. The voltage will be fed straight into the VCO input by the filter, which modifies the frequency accordingly. The VCO output frequency is equal to the input signal frequency when the circuit is locked. Its phase difference is continuous. When a phase mismatch occurs, the voltage leaving the phase capacitor rises. The frequency is adjusted to control the VCO operation. It is increased until the phase gap between the two signals decreases, at which point it is locked. As a result, the VCO output signal is always consistent in size. The phase of the incoming signal will always

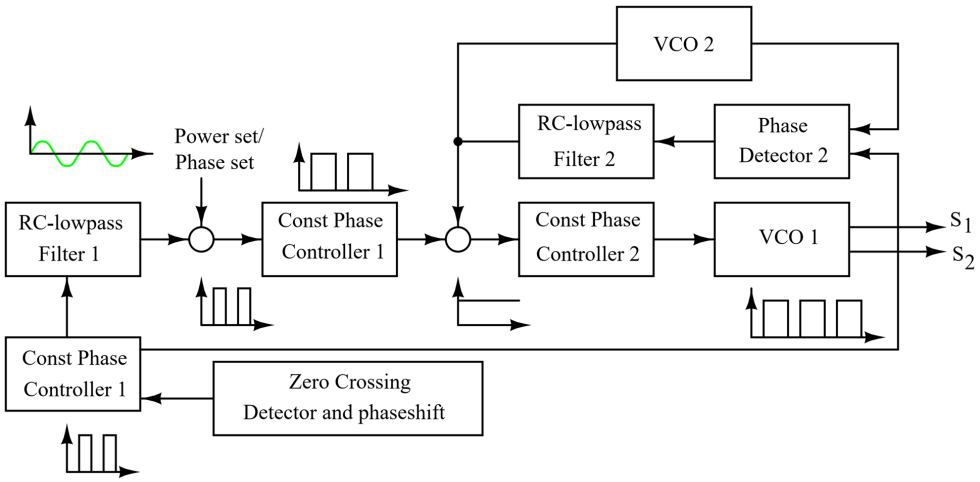

Fig. 4: *Block diagram of control switching S_1 and S_2.*

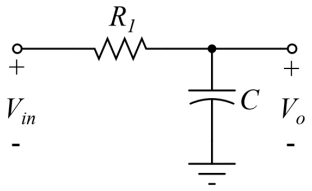

Fig. 5: *Circuit of the lowpass filter.*

affect the frequency value. In the mathematical model of a phase-locked loop, the output phase is set to the input phase. The VCO output frequency is controlled by the output signal of the low pass filter, shifting it away from the middle frequency ($\Delta\omega$), as expressed by

$$\Delta\omega(s) = K_0 \cdot V_c(s) \tag{8}$$

$$\omega = \frac{d\theta}{dt} \tag{9}$$

The output angle of the phase-locked loop can be derived from Eqs. (8) and (9). Thus, it can be written as

$$\frac{d\theta_o}{dt} = K_0 \cdot V_c(s) \tag{10}$$

$$\theta_o(s) = \frac{K_0 \cdot V_c(s)}{s} \tag{11}$$

2.4 RC Lowpass Filter

The first-order RC lowpass filter circuit is depicted in Fig. 5, with the voltage generated by the phase components and used to compare the output voltage to the desired phase order. The transfer function of the RC lowpass filter is

$$F(s) = \frac{1}{1 + R_1 C s}. \tag{12}$$

The output signal is determined from the transfer function when the input signal is applied to the RC lowpass filter as

$$\frac{\theta_o(s)}{\theta_i(s)} = \frac{\frac{K_d K_0}{R_1 C}}{s^2 + \frac{s}{R_1 C} + \frac{K_d K_0}{R_1 C}}. \tag{13}$$

Eq. (13) has a lower term, identical to the standard form of transfer function for a second-order system

$$s^2 + 2\zeta\omega_n s + \omega_n^2 = 0. \tag{14}$$

The natural frequency (ω_n) of the loop and the damping factor (ζ) can be identified by

$$\omega_n = \sqrt{K_d K_0 \omega_{LPF}} \tag{15}$$

$$\zeta = \frac{1}{2}\sqrt{\frac{\omega_{LPF}}{K_d K_0}} \tag{16}$$

where ω_{LPF} is the cut off frequency of the low pass filter circuit. It can be obtained from

$$\omega_{LPF} = \frac{1}{R_1 C}. \tag{17}$$

The various harmonic elements of a rectangular pulse voltage are depicted as

$$V = \frac{4V_1}{\pi} \sum_{n+1}^{\infty} \frac{1 - (-1)^n}{2n} \sin \omega t \tag{18}$$

$$V = V_1\left(\frac{4}{\pi} \sin \omega t + \frac{4}{3\pi} \sin 3\omega t + \frac{4}{5\pi} \sin 5\omega t + \ldots\right). \tag{19}$$

3. EXPERIMENTAL RESULTS

The application was used to simulate the operation using different parameters. It can also be calculated using the inductance coil to simulate working in steady state to figure out how to control the operation of rectifiers and inverters. The magnitude of the voltage and current at different sections of the circuit equipment

Table 1: *Parameters for the hardware setup.*

Parameter	Symbol	Value
Input voltage	v_{AC}	220 V_{rms}
Switching frequency	f_s	45–55 kHz
Resonant capacitor	C_1, C_2	1.5 μF
	C_r	4 μF
Induction coil inductor	L_{coil}	1.98 μH
Load resistor	R_{coil}	45.6 mΩ
Dead time	$T_{deadtime}$	1.5 μs

were examined to ensure the actual operation would not exceed the device rating. The frequency of a three-phase inverter was increased in the simulation by controlling the IGBT signal. The switch operation in each phase was changed to a single waveform, operating at the switching frequency. The parameters for the hardware setup are shown in Table 1. In the design example, the induction coil inductor is 1.98 μH at a switching frequency of 51 kHz, while the resonant capacitor (C_r) can be calculated by $1/(\omega^2 L)$, which is equal to 4 μF.

Fig. 6(a) shows the simulation results of voltage and current waveforms for the switching device with the switch open circuit operating at a frequency higher than the resonant frequency. The voltage drops across it are the same as the DC voltage source, with no current flowing through it. The voltage across the switching device decreases to zero for a closed circuit, and the current flowing through it begins at zero. Since the circuit is in a lagging current, the voltage does not cause a spike in current at the switch device. As a result, there are no switching losses when the device is turned on. This verifies that the switching device is set to zero-voltage switching at turn-on. Fig. 6(b) shows the experimental results of the voltage, current, and power waveforms for the switching device (IGBT). When the IGBT is turned on, the voltage lowers from the rated DC voltage source to zero with no switching losses due to the current flowing into it being near to zero. Depending on the load and switching frequency, the current will then change from zero to the rated current. When the IGBT is turned off, the voltage drops, changing from zero to the rated voltage, while the current returns to zero. The switching losses in this circumstance are approximately equal to 17 W.

Fig. 7 illustrates the voltage and current output waveforms of the inverter at the primary coil in the high frequency transformer. The current waveform is sinusoidal in shape, and the voltage waveform rectangular. The voltage leading the current has a phase angle of around 10 degrees. The voltage and current output waveforms in the experimental results are similar to the simulation. The average power of the output inverter is approximately equal to 724 W.

Following the design, the values were used to simulate the operation of the prototype using an emulator before building the actual machine and adjusting it to the

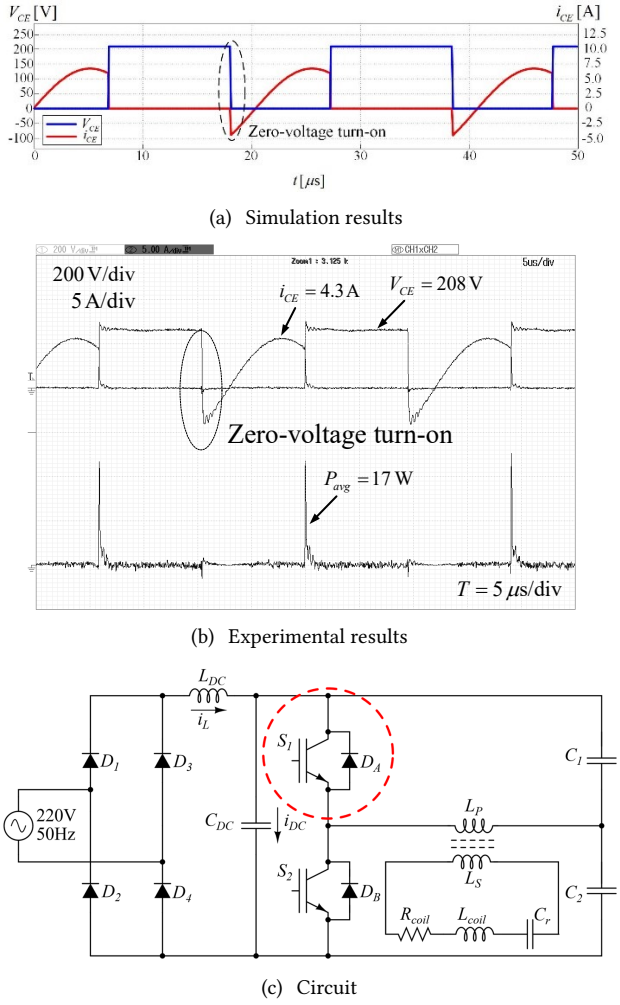

(a) Simulation results

(b) Experimental results

(c) Circuit

Fig. 6: *Waveforms of V_{CE} and i_{CE} on the switch device.*

appropriate setting using the simulation results for the voltage and current flowing through the switches of the inverter circuit. The simulation of voltage and current as well as the analysis of the results from the supply of the output voltage to the half-bridge inverter circuit can be observed on the output side of the inverter circuit.

The goal of simulation is to verify that the power control circuit is operating properly and the power can be modified by adjusting the load current. This procedure controls the inverter to operate at a higher resonant frequency at all times, and at a frequency close to the resonant frequency at which the load receives the highest current. When the inverter operation is considerably greater than the resonant frequency in the phase of the leading current or lagging mode, the load current will progressively decrease.

Only the fundamental harmonic influence is considered when the pulse voltage magnitude is thought to be at the resonant frequency. It can be expressed as

$$V_{1,rms} = \frac{4V_m}{\pi\sqrt{2}}. \tag{20}$$

Therefore, the induction coil power of the output inverter

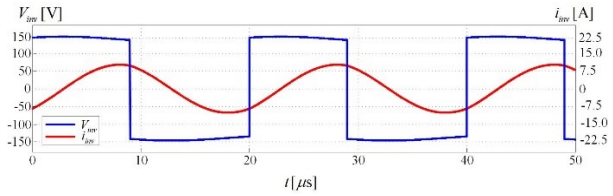

(a) Simulation results

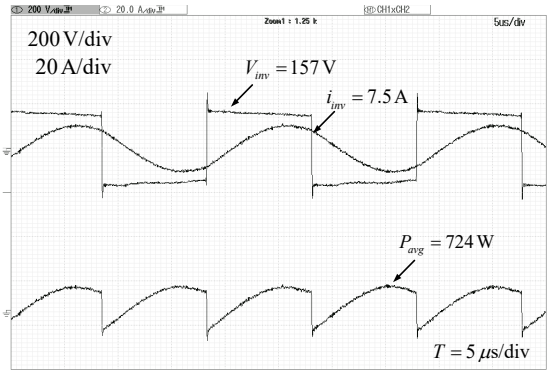

(b) Experimental results

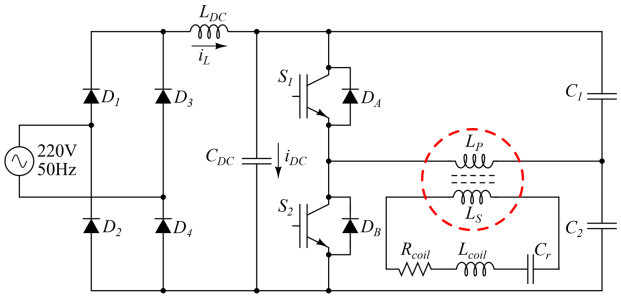

(c) Circuit

Fig. 7: *Waveforms of V_{inv} and i_{inv} at the output of the inverter.*

is calculated by

$$P_{coil} = \frac{V_{1,rms}^2}{R_s} \tag{21}$$

$$P_{coil} = \frac{P_W}{\eta}. \tag{22}$$

The induction coil power can also be determined by entering the current into the induction coil as

$$P_{coil} = I_{coil,rms}^2 R_s. \tag{23}$$

Therefore, Eq. (23) can be used to obtain the RMS of the induction coil current as

$$I_{coil,rms} = \sqrt{\frac{P_{coil}}{R_s}}. \tag{24}$$

Figs. 8 and 9 illustrate the experimental results for the voltage, current, and average power of the inverter measured at the primary induction coil (L_P). During a switching frequency of 53 kHz, the voltage, current, and average power are 159 V, 5.15 A, and 300 W, respectively.

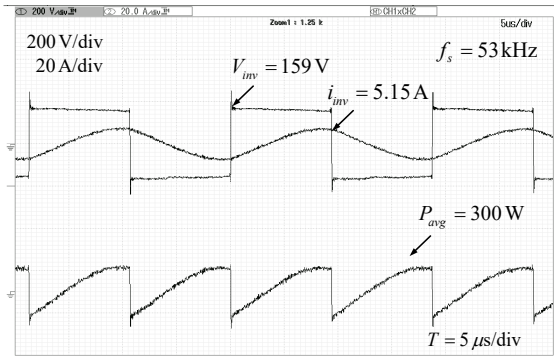

Fig. 8: *Waveforms of voltage, current, and average power for the output inverter at a switching frequency of 53 kHz.*

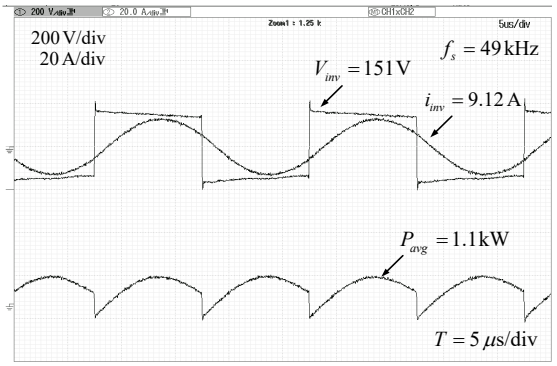

Fig. 9: *Waveforms of voltage, current, and average power for the output inverter at a switching frequency of 49 kHz.*

While during a switching frequency of 49 kHz, the voltage, current, and average power are 151 V, 9.12 A, and 1.1 kW, respectively. Therefore, according to Eqs. (23) and (24), the current and average power are affected by the switching frequency. As can be observed, the change in current and average power is inversely proportional to the switching frequency.

Fig. 10 shows the current and voltage waveforms at the inductor coil, where the phase angle of the voltage precedes the current at almost 90 degrees. From the experimental results, the phase angle of the current and load voltage can be kept constant throughout the heating of the workpiece. The temperature of the load parameter increases when the workpiece heats up, as evidenced by the change in input current, while the input voltage remains constant, resulting in the resonant frequency. Hence, the circuit has a value that changes accordingly. According to the results of previous experiments, in the range between room temperature and 700 ℃, the load resistance was not much different. As a result of this experiment, the current was supplied to the resonant circuit at different temperatures.

The process begins with a control test on the protected unit by cutting off the gate drive signal when a fault occurs. Upon completion of overcurrent testing at IGBT, it was established that the gate would be cut off immediately to prevent IGBT from being damaged by overcurrent and all operations then stop. When the

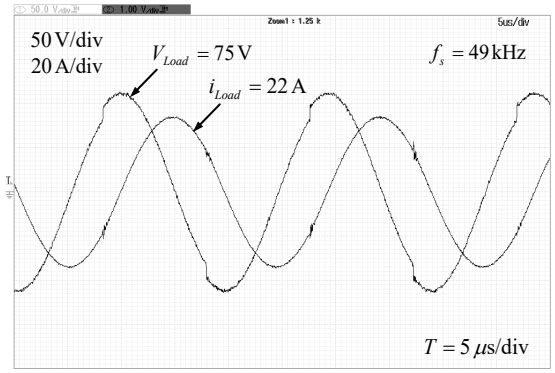

(a) Experimental results

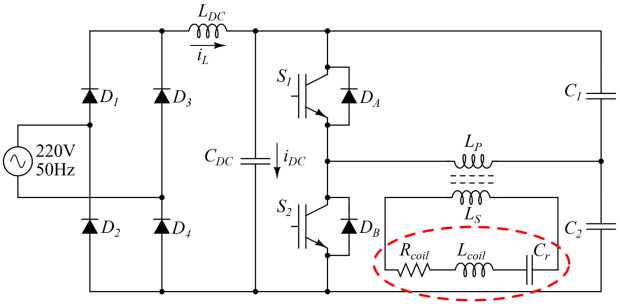

(b) Circuit

Fig. 10: *Waveforms of voltage and load current at a switching frequency of 49 kHz.*

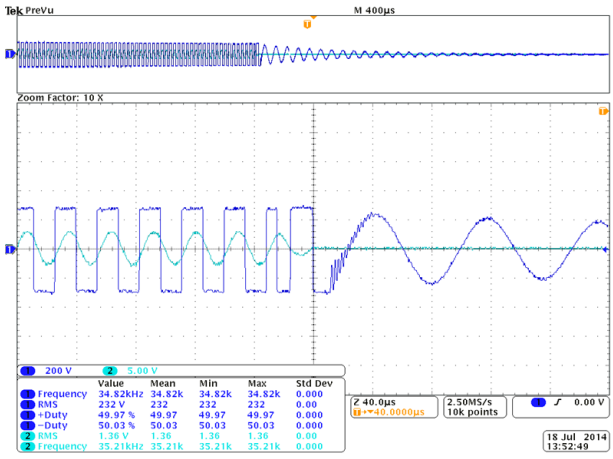

Fig. 11: *The output signal of the current and voltage after protection is activated.*

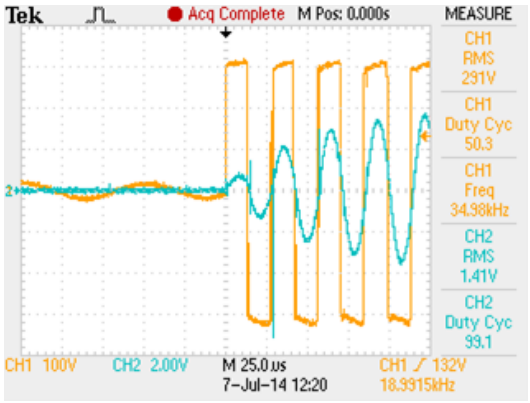

(a)

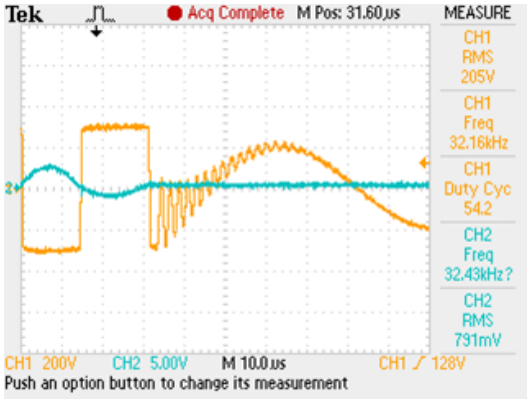

(b)

Fig. 12: *Waveforms of the output current and voltage; (a) switch is connected and (b) switch is disconnected.*

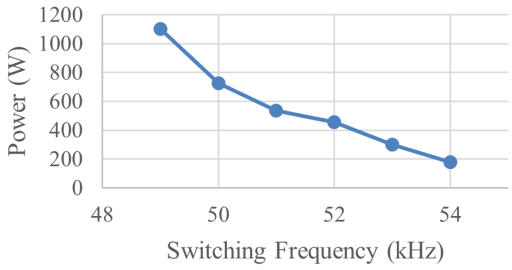

Fig. 13: *Relationship between the power and switching frequency of the inverter.*

water supply to the inductor coil stops, the gate lead signal is cut off immediately to prevent the extreme heat generated by the current flowing into the coil and causing a short circuit. From the experiment, it was established that if the temperature rise in the IGBT exceeds the setting value, the gate signal would be cut off immediately. Finally, during testing, when the capacitor voltage rises above a predetermined value, the gate signal cuts off immediately. Fig. 11 shows the output signal of the current and voltage after protection has been activated. Fig. 12 shows the output voltage and current waveforms, amplified to clearly show the disconnection and connection of switches in the power circuit.

Fig. 13 presents a graph of the relationship between the power and switching frequency of the inverter. The induction machine produces the most power when the operating frequency at the inverter is close to the resonant frequency. This circuit demonstrates efficiency of approximately 91.67%. The power will be lower if the switching frequency of the inverter is higher than the resonant frequency. The frequency used in the experiment is 49–54 kHz. Thus, the temperature of the workpiece can be adjusted by changing the switching frequency to correspond to the current and power values. The measured voltage, current, and power of the inverter

Table 2: *Voltage, current, and power of the inverter.*

f_s (kHz)	V_{inv} (V)	i_{inv} (A)	P_{avg} (W)
49	151	9.12	1,100
50	158	7.50	724
51	159	6.69	535
52	159	6.07	454
53	159	5.15	300
54	159	4.16	180

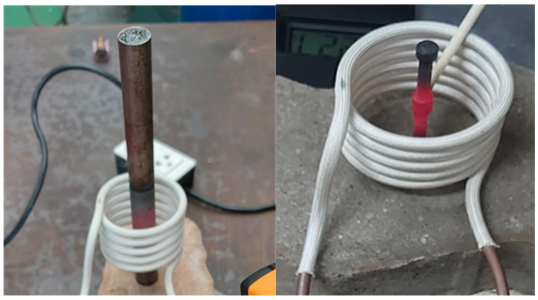

Fig. 14: *Experimental results for heating a tensile workpiece measuring 45 mm and 5 mm in diameter.*

are illustrated in Table 2. Furthermore, the experimental results for heating a tensile workpiece measuring 45 mm in length and 5 mm in diameter are displayed in Fig. 14.

4. CONCLUSION

This paper proposed a prototype design for a 1.5 kW induction heater with a half-bridge inverter circuit voltage-source. In summary, three specimens measuring approximately 3, 5, and 10 mm in diameter and roughly 50 and 70 mm in length were analyzed. The inverter operating at the phase angle of the current lag voltage was approximately 10 degrees. The switch of the inverter operated at a slightly higher frequency than the resonant frequency. At a switching frequency of less than the resonant frequency, loss occurred during the IGBT connection, due to the presence of current at the start of the circuit causing a high peak current at the switch. However, at a higher switching frequency than the resonant frequency, no loss occurred, while the IGBT continued the circuit because it started with a zero current. Consequently, it was preferable to operate the inverter at a switching frequency slightly higher than the resonant frequency. In this paper, the frequency changed between 45 and 55 kHz according to the load conditions and the inverter continued to operate. Conclusively, the induction heating machine for tensile testing provides over-temperature, overvoltage, water circuit, and overcurrent protection systems. Furthermore, the half-bridge voltage-source inverter circuit offers adjustable pulse density control. Finally, with a 1.5 kW input power rating, the inverter operates at a switching frequency above the resonant frequency of 30–40 kHz. Therefore, the proposed prototype system provides practical protection in terms of induction heating.

REFERENCES

[1] J. Davies and P. Simpson, *Induction Heating Handbook*. New York, NY, USA: McGraw-Hill, 1979.

[2] S. Chudjuarjeen and C. Koompai, "A high-frequency induction cooker using qusai-resonant converter," in *2007 4th International Conference on Electrical Engineering/Electronics, Computer, Telecommunications and Information Technology (ECTI-CON 2007)*, 2007, pp. 378–381.

[3] S. Chudjuarjeen and C. Koompai, "Asymmetrical control with phase lock loop for induction cooking appliances," in *2008 5th International Conference on Electrical Engineering/Electronics, Computer, Telecommunications and Information Technology (ECTI-CON 2008)*, 2008, pp. 1013–1016.

[4] S. Chudjuarjeen, A. Sangswang, and C. Koompai, "LLC resonant inverter for induction heating with asymmetrical voltage-cancellation control," in *2009 IEEE International Symposium on Circuits and Systems*, 2009, pp. 2874–2877.

[5] A. Polsripim, S. Chudjuarjeen, A. Sangswang, P. N. N. Ayudhya, and C. Koompai, "A soft switching class d current source inverter for induction heating with ferromagnetic load," in *2009 International Conference on Power Electronics and Drive Systems (PEDS)*, 2009, pp. 877–881.

[6] Y. Samart, C. Panithan, S. Chudjuarjeen, A. Sangswang, and C. koompai, "An automatic half-bridge resonant inverter with three-phase three-switch buck-type rectifier," in *2010 IEEE Energy Conversion Congress and Exposition*, 2010, pp. 2172–2176.

[7] S. Chudjuarjeen, A. Sangswang, and C. Koompai, "An improved LLC resonant inverter for induction-heating applications with asymmetrical control," *IEEE Transactions on Industrial Electronics*, vol. 58, no. 7, pp. 2915–2925, Jul. 2011.

[8] J. Jittakort, S. Yachiangkam, A. Sangswang, S. Naetiladdanon, C. Koompai, and S. Chudjuarjeen, "A variable-frequency asymmetrical voltage-cancellation control of series resonant inverters in domestic induction cooking," in *8th International Conference on Power Electronics - ECCE Asia*, 2011, pp. 2320–2327.

[9] J. Jittakort, A. Sangswang, S. Naetiladdanon, S. Chudjuarjeen, and C. Koompai, "LCCL series resonant inverter for ultrasonic dispersion system with resonant frequency tracking and asymmetrical voltage cancellation control," in *41st Annual Conference of the IEEE Industrial Electronics Society (IECON 2015)*, 2015, pp. 2491–2496.

[10] S. Yachiangkam, A. Sangswang, S. Naetiladdanon, C. Koompai, and S. Chudjuarjeen, "Steady-state analysis of ZVS and NON-ZVS full-bridge inverters with asymmetrical control for induction heating applications," *Journal of Power Electronics*, vol. 15, no. 2, pp. 544–554, Mar. 2015.

[11] J. Jittakort, A. Sangswang, S. Naetiladdanon,

C. Koompai, and S. Chudjuarjeen, "Full bridge resonant inverter using asymmetrical control with resonant-frequency tracking for ultrasonic cleaning applications," *Journal of Power Electronics*, vol. 17, no. 5, pp. 1150–1159, Sep. 2017.

[12] S. Nilboworn, K. Mahamad, W. Sangchay, and P. Kongrueang, "Edge effect and its influence on the adjacent cavities in a composite insulator," *UTK Research Journal*, vol. 14, no. 1, pp. 23–29, 2020.

[13] C. Wisassakwichai, P. Phaochoo, E. Anusurain, C. Kamonkhantithorn, W. Methavithit, and W. Sirichanon, "Database building with microsoft excel for voltage drop calculation according to thai electrical code 2013 with c++ builder," (in Thai), *UTK Research Journal*, vol. 12, no. 2, pp. 119–135, 2018.

[14] B. Sriboonreung, "Two output power control of induction cooker with full bridge inverter controlled by asymmetrical voltage control," (in Thai), *UTK Research Journal*, vol. 13, no. 2, pp. 1–12, 2019.

[15] J. Ekburanawat, "Full bridge switching power supply for a thermoelectric dehumidifier," (in Thai), *UTK Research Journal*, vol. 13, no. 2, pp. 54–64, 2019.

[16] A. Dominguez, L. A. Barragan, J. I. Artigas, A. Otin, I. Urriza, and D. Navarro, "Reduced-order models of series resonant inverters in induction heating applications," *IEEE Transactions on Power Electronics*, vol. 32, no. 3, pp. 2300–2311, Mar. 2017.

[17] J. Villa, J. I. Artigas, J. R. Beltran, A. D. Vicente, and L. A. Barragan, "Analysis of the acoustic noise spectrum of domestic induction heating systems controlled by phase-accumulator modulators," *IEEE Transactions on Industrial Electronics*, vol. 66, no. 8, pp. 5929–5938, Aug. 2019.

[18] A. G. Kothalkar and M. A. Ahire, "Hot tensile test-a literature review," *International Journal of Modern Trends in Engineering and Research*, vol. 2, no. 7, pp. 1772–1776, Jul. 2015.

[19] M. Ganapathy, N. Li, J. Lin, M. Abspoel, and D. Bhattacharjee, "A novel grip design for high-accuracy thermo-mechanical tensile testing of boron steel under hot stamping conditions," *Experimental Mechanics*, vol. 58, no. 2, pp. 243–258, Feb. 2018.

Saichol Chudjuarjeen received his B. Eng. degree in electrical engineering from Mahanakorn University of Technology (MUT), Thailand in 2000, M. Eng. degree in electrical engineering, and Ph.D. degree in electrical and computer engineering from King Mongkut's University of Technology Thonburi (KMUTT), Thailand in 2004 and 2011, respectively. He is currently a lecturer in the Department of Electrical Engineering, Rajamangala University of Technology Krungthep, Thailand. His research interests mainly involve high frequency resonant inverters for induction heating, current source and voltage source inverters, and control of power electronic systems.

Nathabhat Phankong received his B. Eng. (second-class honors) and M. Eng. degrees in electrical engineering from King Mongkut's University of Technology Thonburi (KMUTT), Thailand in 1999 and 2003, respectively, and his Ph.D. degree in electrical engineering from Kyoto University, Japan in 2010. He is currently a lecturer in the Department of Electrical Engineering, Rajamangala University of Technology Thanyaburi, Thailand. His research interests are mainly in power electronic systems and conversion.